

## A NUMERICAL STUDY OF THE EFFECTS OF INJECTION RATE SHAPE ON COMBUSTION AND EMISSION OF DIESEL ENGINES

by

**Zhixia HE<sup>a\*</sup>, Tiemin XUAN<sup>b</sup>, Yanru XUE<sup>c</sup>, Qian WANG<sup>a</sup>, and Liang ZHANG<sup>a</sup>**

<sup>a</sup> School of Energy and Power Engineering, Jiangsu University, Zhenjiang, China

<sup>b</sup> CMT – Motores Térmicos, Universidad Politécnica de Valencia,  
Valencia, Spain

<sup>c</sup> Mechanical and Electrical Engineering College, Hebei Normal University of Science & Technology, Qinhuangdao, China

Original scientific paper

DOI: 10.2298/TSCI130810013H

*The spray characteristics including spray droplet sizes, droplet distribution, spray tip penetration length, and spray diffusion angle directly affects the mixture process of fuel and oxygen and then plays an important role for the improvement of combustion and emission performance of diesel engines. Different injection rate shapes may induce different spray characteristics and then further affect the subsequent combustion and emission performance of diesel engines. In this paper, the spray and combustion processes based on four different injection rate shapes with constant injection duration and injected fuel mass were simulated in the software of AVL FIRE. The numerical models were validated through comparing the results from the simulation with those from experiment. It was found that the dynamic of diesel engines with the new proposed hump shape of injection rate and the original saddle shape is better than that with the injection rate of rectangle and triangle shape, but the emission of NO<sub>x</sub> is higher. The soot emission is lowest during the late injection period for the new hump-shape injection rate because of a higher oxidation rate with a better mixture between fuel and air under the high injection pressure.*

Key words: *diesel engine, injection rate shape, combustion and emission, numerical simulation*

### Introduction

Because of outstanding power performance, fuel economy and reliability, the diesel engine is widely used in power systems around the world. As a result of rich oxygen combustion, the CO and HC emissions of the diesel engine are less than that of the gasoline, but the NO<sub>x</sub> emissions are at the same level and particulate matter emissions for diesel engines are produced over dozens of times than that of gasoline engines [1]. In this way nowadays, various new strategies, like high pressure common rail injection system [2, 3], Turbocharging technology [4, 5], EGR technology [6, 7], etc., have been used to reduce the emissions of NO<sub>x</sub> and particulate matter. However, the engine researchers still continue to face the new challenges to meet the requirements of the increasingly stringent emission regulations.

It is extremely complicated for the fuel spray in diesel engines, involving the droplet breakup, atomization, evaporation, collision and other physical and chemical processes. For the

---

\* Corresponding author; e-mail: zxhe@ujs.edu.cn

DI diesel engine, the fuel will be directly injected into the combustion chamber and the fuel injection characteristics is one of the keys to control the mixing of fuel and air and then will play an important role in combustion processes. Scholars have done a lot of research on the effect of fuel injection characteristics on combustion and emission of diesel engines. Badami *et al.* [8] carried out experiments on a DI diesel engine of a passenger vehicle to analyze the effect of different injection strategies on the emission, combustion noise and fuel consumption. It was found that it is helpful to reduce combustion noise and fuel consumption for two pilot injections but with higher emission. It could reduce the soot emission with post injection but need to optimize the injection timing. Suh [9] investigated multiple injection strategies for the improvement of combustion and exhaust emissions characteristics in a low compression ratio engine. It was observed that two pilot injections can improve combustion efficiency and help the engine operate more stably which lead to remarkable reduction of  $\text{NO}_x$  and soot emissions compared to the single injection. Sayin *et al.* [10] studied the effect of injection timing on the exhaust emissions of a diesel engine using diesel-methanol blends. It was found that advancing injection timing improves the reaction of fuel and air mixture which led to lower CO and higher  $\text{CO}_2$ . Also  $\text{NO}_x$  emission will be increased with advancing of injection timing because of the much higher temperature in cylinder owing to the start of the ignition was advanced. The effect of fuel injection pressure on combustion and emissions characteristics of a single-cylinder diesel engine was investigated by Agarwal [11] *et al.* who demonstrated that cylinder pressure and heat release rate will be higher for lower fuel injection pressure while  $\text{CO}_2$  and HC emissions are decreased and  $\text{NO}_x$  emissions are increased with increase of fuel injection pressure.

Besides all above factors, fuel injection rate shape may also have a great influence on spray characteristics and then further largely affect the combustion and emission characteristics, which have been studied by many researchers all over the world. Desantes *et al.* [12, 13] performed experiment to study the effects of different boot-type injection rate shape on the combustion and emissions of a heavy-duty diesel engine. Their results showed that as the boot-type shape length corresponding to the period of injection is increased or the boot-type shape height with injection rate is reduced,  $\text{NO}_x$  emissions will be obviously reduced but fuel consumption and soot emissions will be increased because of much more diffusion combustion and less pre-mixed combustion. Based on the KIVA-CHEMKIN computational fluid dynamics code, Shuai *et al.* [14] used an improved spray model to simulate the effect of seven different injection rate shapes on low-temperature combustion. It was concluded that the injection rate shape are less important for early injection than for late injection case and rectangle-type and boot-type injection rate shapes have the potential to decrease the soot, HC and CO emissions compared to other rate shapes. The effect of boot-type injection rate shape and top-hat shape on combustion and emissions of diesel engines were compared in experiments by Luckhchoura [15] who found that boot-type injection rate shape shows a strong potential to improve combustion noise and simultaneously decrease soot and CO emissions at exhaust valve opening for constant  $\text{NO}_x$  emissions, compared top-hat shape.

Although some experimental studies have been reported and various injection parameters and injection rate shapes have been examined to achieve low temperature combustion and low emissions; the data from experiments is quite few. The numerical simulation method has been another effective tool for revealing much more details while there have been relatively few detailed computational studies dealing with these aspects and the influence mechanism is not very clear. In this paper, a four-cylinder GM diesel engine was simulated to analyze the effects of four different fuel injection rate shapes on the combustion and emissions.

## Numerical approach

### Calculating meshes

The physical model was from a 1.9 L, 4-cylinder GM diesel engine with a 7-hole common-rail injector of Argonne National Laboratory [16]. Its structure parameters and experimental condition parameters are shown in tab.1 and the fuel injection system parameters are shown in tab. 2.

For the spray and combustion simulation, because of the symmetrical location of the injector at the center of the combustion chamber and proportional spacing location of the injector holes along circumference, the CFD calculations were performed with the mesh of 51.43° sector zones. Figure 1 shows the grids at bottom dead center (BDC) and top dead center (TDC), respectively. According to grid independence analysis, the computational zone has 71026 (BDC) computational cells.

To reduce the calculation time, the intake stroke and exhaust stroke was not taken into account. Calculations begin at intake valve closure (IVC = 218.5°) and end at exhaust valve opening (EVO = 483°). The initial conditions and fuel injection rate are shown in tab. 3 and fig. 1, respectively.

**Table 3. Initial conditions**

Parameters	Value
Gas pressure at IVC [MPa]	0.123
Gas temperature at IVC [K]	310
Swirl ratio	2.37
Turbulent kinetic energy [ $m^2s^{-2}$ ]	12.36
Turbulent length scale [m]	0.00513
Oxygen concentration	21%

**Table 1. Engine specifications**

Engine	GM
Bore/stroke [mm]	82/90.4
Connection rod length [mm]	145.4
Engine speed [rpm]	1500
Compression ratio	16.8
Fuel	$C_7H_{16}$

**Table 2. Injection system specifications**

Parameters	Value
Mass of fuel injected/injector/nozzle [kg]	$1.2495 \cdot 10^{-6}$
Spray cone angle [°]	9
Nozzle position [mm]	1.16
Spray angle [°]	148
Injection duration [°]	8.5
Nozzle hole diameter [mm]	0.141

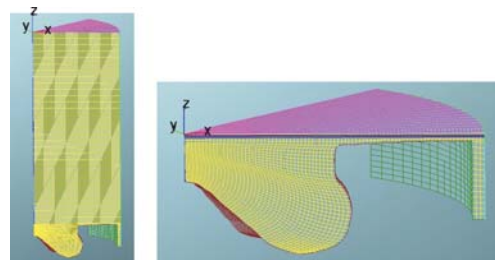


**Figure 1. The grid of combustion chamber at BDC (left) and TDC (right)**

## Numerical models

### Turbulence model

The  $k-\zeta-f$  four equations model was used in this paper for modeling of turbulence. This model has been recently developed by Hanjalic, *et al.* [17]. The authors proposed a version of eddy-viscosity model based on Durbin's elliptic relaxation concept [18] in order to improve numerical stability of the original model by solving a transport equation for the velocity scale ratio  $\zeta = \bar{v}^2/k$  instead of velocity scale  $\bar{v}^2$  [19]. The full model is given as follows:

The eddy-viscosity is obtained from:

$$v_t = C_\mu \zeta \frac{k^2}{\varepsilon} \quad (1)$$

and the rest of variables can be got from the following set of model equations as:

$$\rho \frac{Dk}{Dt} = \rho(P_k - \varepsilon) + \frac{\partial}{\partial x_j} \left[ \left( \mu + \frac{\mu_t}{\sigma_k} \right) \frac{\partial k}{\partial x_j} \right] \quad (2)$$

$$\rho \frac{D\varepsilon}{Dt} = \rho \frac{C_{\varepsilon 1}^* P_k - C_{\varepsilon 2} \varepsilon}{T} + \frac{\partial}{\partial x_j} \left[ \left( \mu + \frac{\mu_t}{\sigma_k} \right) \frac{\partial \varepsilon}{\partial x_j} \right] \quad (3)$$

$$\rho \frac{D\zeta}{Dt} = \rho f - \rho \frac{\zeta}{k} P_k + \frac{\partial}{\partial x_j} \left[ \left( \mu + \frac{\mu_t}{\sigma_k} \right) \frac{\partial \zeta}{\partial x_j} \right] \quad (4)$$

where,  $f$  can be calculated with the equation:

$$f = L^2 \frac{\partial^2 f}{\partial x_j \partial x_j} \left( C_1 + C_2 \frac{P_k}{\zeta} \right) \frac{\left( \frac{2}{3} - \zeta \right)}{T} \quad (5)$$

and the turbulent time scale  $T$  and length scale  $L$  are given by:

$$T = \max \left[ \min \left( \frac{k}{\varepsilon}, \frac{a}{\sqrt{6} C_\mu^v |S| \zeta} \right), C_T \sqrt{\frac{v^3}{\varepsilon}} \right] \quad (6)$$

$$L = C_L \max \left[ \min \left( \frac{\sqrt{k^3}}{\varepsilon}, C_\eta \frac{\sqrt[4]{v^3}}{\sqrt[4]{\varepsilon}} \right) \right] \quad (7)$$

Additional modifications to the equation is that the constant is dampened close to the wall, thus:

$$C_{\varepsilon 1}^* = C_{\varepsilon 1} \left( 1 + 0.045 \sqrt{\frac{1}{\zeta}} \right) \quad (8)$$

The four-equation  $k$ - $\zeta$ - $f$  model is very robust and more accurate than the simpler two-equation eddy viscosity models. On average, the computing time is increased by up to 15% when compared with the computing time needed for the  $k$ - $\varepsilon$  model calculations [20].

### Spray break-up model

The KH-RT (Kelvin-Helmholtz Rayleigh-Taylor) model was applied for modeling of spray break-up process in this paper. Droplets within the break-up length are considered to undergo only KH break-up, whereas in the further downstream far field, both KH and RT mechanisms exist [21]. The KH mechanism is favored by high relative velocities and high ambient density. The WAVE model equations were used to simulate the KH break-up [22]. The RT mechanism is driven by rapid deceleration of the droplets causing growth of surface waves at the droplet stagnation point. The RT disturbances are described by the fastest growing frequency  $\Omega_{RT}$  and the corresponding wave number  $K_{RT}$ :

$$\Omega_{RT} = \sqrt{\frac{2}{3\sqrt{3}\sigma} \frac{g_t |\rho_p - \rho_g|^{1.5}}{\rho_p + \rho_g}} \quad (9)$$

$$K_{RT} = \sqrt{\frac{g_t |\rho_p - \rho_g|}{3\sigma}} \quad (10)$$

Here  $\rho_p$  is the density of the droplet,  $\rho_g$  is the density of gas,  $g_t$  – the deceleration in the direction of travel  $g_t = (3/8)C_D(\rho_g U_{rel}^2)/\rho_p r$ .

**Combustion and emission models**

The ECFM-3Z model was applied for combustion. The ECFM-3Z model was developed by the consortium groupement scientifique moteurs (GSM) specifically for diesel combustion [23]. This model is based on a flame surface density transport equation and a mixing model that can describe inhomogeneous turbulent premixed and diffusion combustion. The model relies on the ECFM combustion model, previously described on a three areas mixing description. In the ECFM-3Z model, the transport equations are solved for the averaged quantities of chemical species  $O_2$ ,  $N_2$ ,  $CO_2$ ,  $CO$ ,  $H_2$ ,  $H_2O$ ,  $O$ ,  $H$ ,  $N$ ,  $OH$ , and  $NO$ . Here, averaged means these quantities are the global quantities for the three mixing zones (that is in the whole cell). Therefore, the term “burnt gases” includes the real burnt gases in the mixed zone (zone  $F_b$  in fig. 2) plus a part of the unmixed fuel (zone  $M_b$  in fig. 2) and air (zone  $A_b$  in fig. 2).

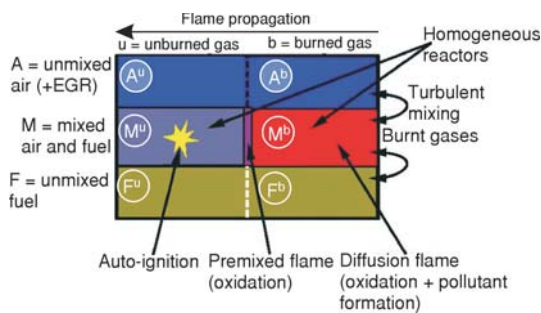


**Figure 2. Zones in ECFM-3Z Model**

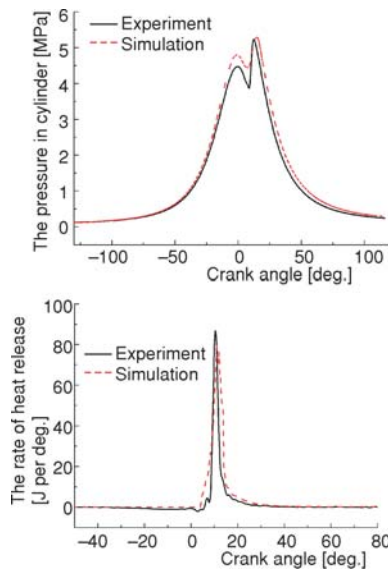


**Figure 3. Comparisons of pressure and heat release rate between experiment and simulations**

The extended Zeldovich model was used for  $NO_x$  formation and Frolov kinetic model for soot formation and oxidation. The basis of the Frolov kinetic model is a detailed chemical reaction scheme for the calculation of soot formation and oxidation. It includes the mechanisms of formation of polyaromatic hydrocarbons and polyynes, the mechanisms of soot precursor formation due to condensation of polyaromatic and polyyn molecule, soot particle growth by the reactions of HACA mechanism and polyyn molecule addition, the mechanism of acetylene pyrolysis and pure carbon cluster formation, as well as the reactions of hydrocarbon (n-heptane) oxidation [24-30].

**Model validation**

Using above numerical models, the simulations of in-cylinder combustion and emission of this diesel engine were performed with the assumption of uniform temperature of 413 K for the cylinder wall, the temperature of 553 K for the cylinder head, and 593 K for the piston top. Experiments for this GM diesel model were performed at Argonne National Laboratory and the data is from the reference [16]. Figure 3 shows the comparisons between the predicted and measured in-cylinder pressure

and heat release rate of single-injection at full load and the speed of 1500 rpm. It can be seen that both the in-cylinder pressure curve and heat release rate curve predicted with these models are reasonably close to those from the experiment.

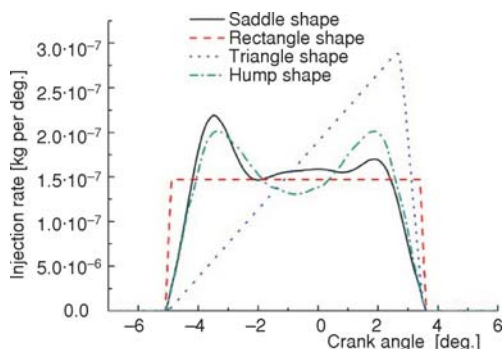


**Figure 4. Four different types of injection rate shape**

diesel engine in that paper. It was found the indicated mean effective pressure of the “hump mode” with four injections was higher than other injection modes and the results of the emissions were better. The hump shape with four injections was carried out in one injection rate in this paper and it is an ideal injection rate.

#### ***Effect of injection rate shapes on ignition delay and heat release rate***

The fuel is injected out of the nozzle hole and into the cylinder and then will go through some physical and chemical preparation processes before combustion, like atomization, evaporation, diffusion, and mixing with air during ignition delay period. It is the ignition delay period that will directly affect the level of premixed combustion and determine the peak cylinder pressure,

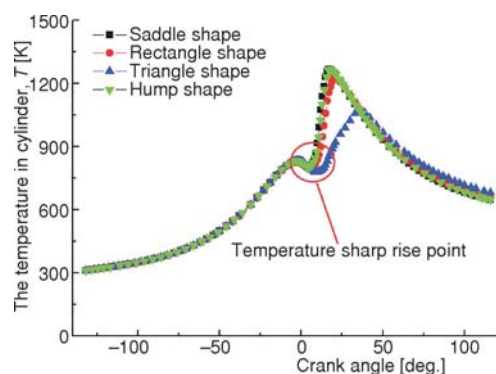


**Figure 5. Temperature in cylinder for different injection rate shapes**  
(for color image see journal web site)

#### **Results and discussions**

As above mentioned, the fuel injection rate greatly affects the combustion and heat release processes of diesel engines, as well as the emission and engine performance. In this paper, four types of injection rate shape (hump shape, original saddle shape, the rectangle and triangle shape) with constant injection duration and the same mass of fuel injected were selected for the study of the effect of the different injection rate shapes on combustion and emission characteristics, as shown in fig. 4. The original saddle shape was taken from the reference [16]. The idea of the hump injection rate shape was derived from the reference [31]. The effects of different multi-pulse modes were investigated in a

dieel engine in that paper. It was found the indicated mean effective pressure of the “hump mode” with four injections was higher than other injection modes and the results of the emissions were better. The hump shape with four injections was carried out in one injection rate in this paper and it is an ideal injection rate.

pressure, the peak pressure rise rate and combustion noise. In a word, the ignition delay has a significant influence on the combustion.

Determining of the start of ignition is quite important for getting the ignition delay period. Many methods such as cylinder pressure sharp rise point method, the rate of pressure rise turning point method, cylinder temperature sharp rise point method have been used to determine the start of ignition in the past years [32]. The temperature sharp rise point method was adopted in this paper. Figure 5 shows the temperature curves for different injection rate shapes. The start of ignition and ignition delay period are given in tab. 3.

**Table 3. Start of ignition and ignition delay period for different injection rate shape**

Injection rate shape	Saddle shape	Rectangle shape	Triangle shape	Hump shape
Start of injection [°]	-5.0	-5.0	-5.0	-5.0
Start of ignition [°]	5.2	6.6	9.6	5.4
Ignition delay period [°]	10.2	11.6	14.6	10.4

The ignition delay periods for saddle shape and hump shape are short because of the more injected fuel and higher injection velocity at the initial time of the fuel injection. On the contrary, the ignition delay period for triangle shape is the longest, as shown in tab. 3. It can be seen from fig. 6, the droplet velocity is about 150 m/s at the initial time of injection for the original saddle and hump injection rate shapes, which is higher than that for other two injection rate shapes, especially the triangle shape. It means the initial injection pressure for original saddle and hump injection rate shapes is higher, which contributes to better fuel atomization and evaporation. What is more, the formation time of the premixed gases will be greatly shortened, and then the start of ignition becomes earlier. While the initial injection pressure for triangle injection rate shape is lower and the droplets are too big to evaporate, so the ignition delay becomes longer.

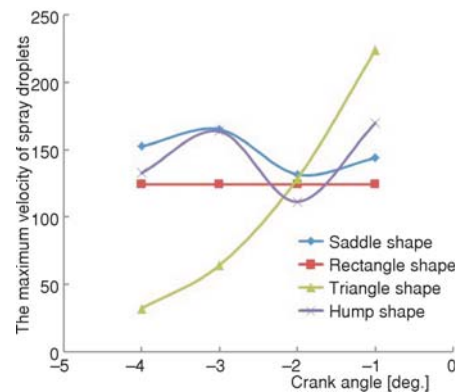


**Figure 6. The maximum of droplet velocity**  
 (for color image see journal web site)

Figures 7 and 8 show the heat release rate and cumulative heat release, respectively. As shown in fig. 7, the peak value of the heat release rate for saddle shape and hump shape was largely greater than that for triangle shape and the heat release duration for triangle injection rate shape was the longest. From fig. 8, there was little difference in the total heat release for different injection rate shapes. Besides the fuel injection rate shapes also greatly affect the combustion center, which was defined as the crank angle degree when 50% of the heat has been released, and the location of combustion center away from TDC may have a great influence on

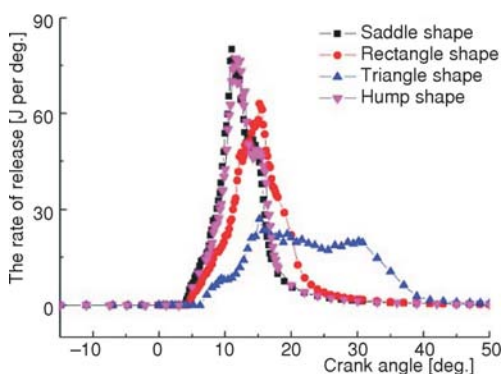


**Figure 7. Heat release rate**  
 (for color image see journal web site)

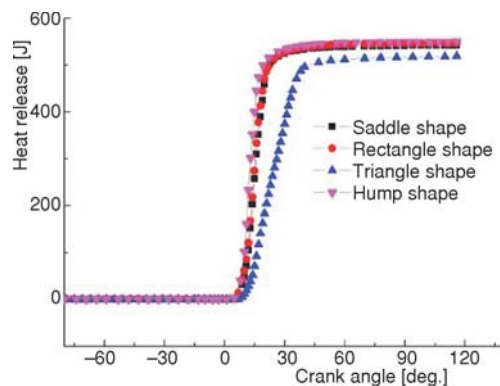


**Figure 8. Total heat release**  
 (for color image see journal web site)

combustion thermal efficiency. The combustion centers for different injection rate shapes are listed in tab. 4.

**Table 4. Combustion center for different injection rate shapes.**

Injection rate shape	Saddle shape	Rectangle shape	Triangle shape	Hump shape
Location of combustion center [°]	12.6	15.0	23.8	12.2

The location of combustion center can be used to show the degree away from the TDC. It can be speculated that the further the combustion center is away from the TDC, the more lost work would be produced in the expansion stroke, so there exists some positive correlation between the lost work and the combustion center. As shown in tab. 4, compared with other three injection rate shapes, the combustion center for hump injection rate shape is the nearest with TDC.

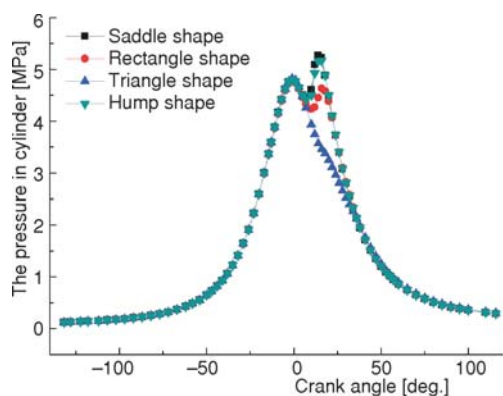


**Figure 9. The mean pressure in cylinder**  
(for color image see journal web site)

The effect of different injection rate shapes on the mean pressure in the cylinder is shown in fig. 9. The peak pressures for saddle shape and rectangle shape are larger than those for other injection rate shapes, which was the result of the higher injection pressure and smaller SMD with better evaporation. Since the higher pressure and rate of pressure release, the engine works quite roughly with much combustion noise [33, 34]. It was concluded that hump injection rate shape performed better in power performance and fuel economy than other injection rate shapes when considering both combustion thermal efficiency and cylinder pressure.

### **Effect of different injection rate shapes on emissions**

High temperature and rich oxygen will be beneficial to the formation of NO, so much more NO will be produced during the period of premixed combustion, where rich oxygen induces a completed combustion and then a higher temperature. Especially when the temperature is above 1800 K, the NO will be produced with exponential increase rate. While a “Freeze” phenomenon corresponding to the NO concentration unchanged will occur with the decrease of exhaust gas temperature during the expansion stroke. Figure 10 shows the NO mass fraction for different injection rate shapes and NO emission is much more for saddle and hump injection rate shapes because of a higher cylinder temperature induced by the higher level of pre-mixed combustion.

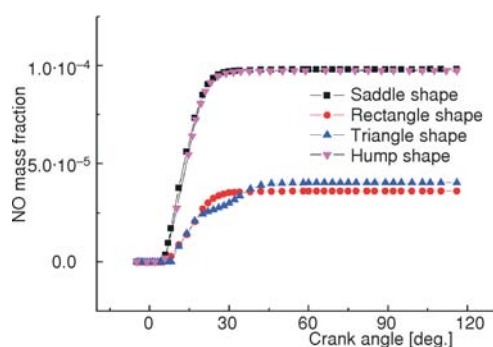


**Figure 10. NO mass fraction for different injection rate shapes**  
(for color image see journal web site)

The generation rate of NO reaches the maximum at about 15° CA for all of the four injection rate shapes. The equivalence ratio, temper-

ature and the NO mass fraction distribution in the diesel engine cylinder for hump and rectangle injection rate shapes are shown in fig. 11. More NO<sub>x</sub> would be produced during the stoichiometric premixed burning ( $\phi \approx 1.0$ ). As shown in fig. 11, there was little difference for the equivalence ratio. However, the high temperature area was larger for hump injection rate shape resulting from higher initial injection pressure and earlier ignition, which then contributed to much more NO emission than that for rectangle rate shape.

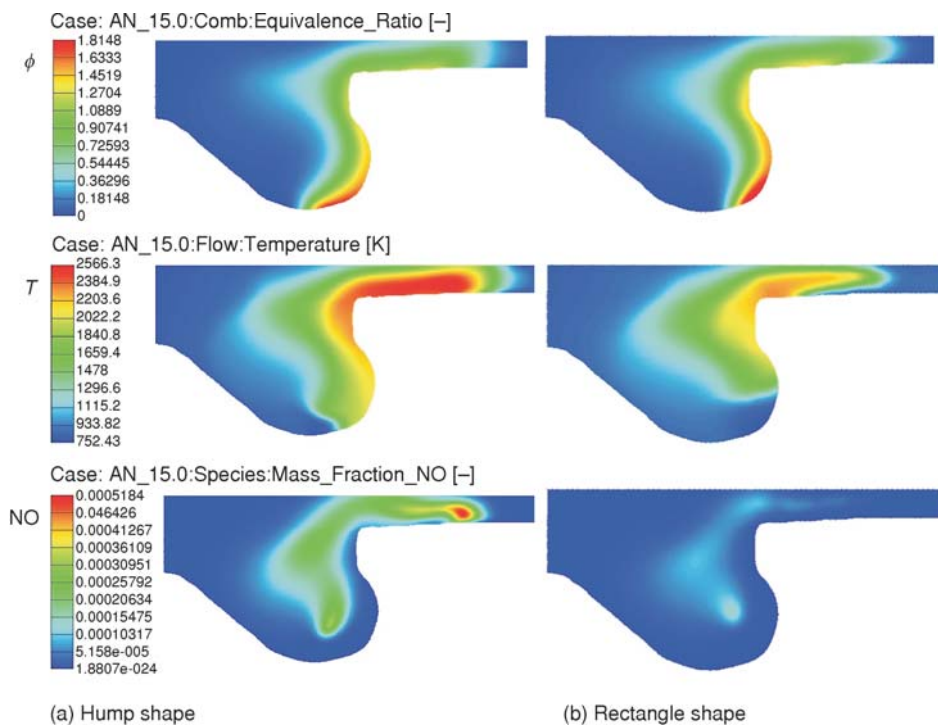


Figure 11. Comparisons between different injection rate shapes at 15° CA (for color image see journal web site)

Soot mass fraction is shown in fig.12 for different injection rate shapes. Soot will be easy to form under the high temperature and low oxygen concentration. In the initial period of combustion, the spray tip burns first and lead to the core of the spray with higher equivalence ratio and fuel spray was surrounded by the flame to make the surrounding with high temperature and low oxygen concentration, which may eventually induce much more soot emission. Therefore more soot was formed for the hump, saddle, and rectangle injection rate shapes with more fuel injected into the chamber during the

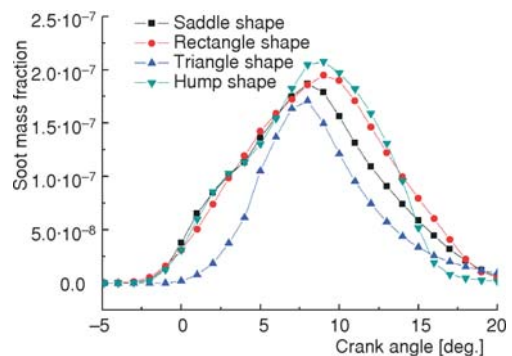


Figure 12. Soot mass fraction for different injection rate shapes

initial period of combustion. As the piston moving down from the TDC, the fuel vapors flowed towards the bottom of the bowl where the high fuel concentration zone would appear. It is another main zone covered by the soot at the end of the combustion, however, the soot would be oxidized and then decrease quickly because of mixing with the fresh air.

Figure 13 shows the distribution of the velocity and the equivalence ratio in the piston bowl at the 15° CA(aTDC). It can be seen from fig.13(a), that the high fuel concentration zone was mainly located in the bowl region. The area of high fuel concentration was a little bigger for hump injection rate shape than that for other injection rate shapes. But the relative concentration for hump injection rate shape was less than that for saddle and rectangle injection rate shapes. As shown in fig. 13(b), the flow velocity for hump injection rate shape was higher than that for the others at the bowl of the piston and there was a obvious back flow which improved the mixture between fuel and air and the oxidation of soot well. As to hump injection rate shape, the oxidation rate of soot was faster than that for the other injection rate shapes at the end of the injection which leads to less soot formation.

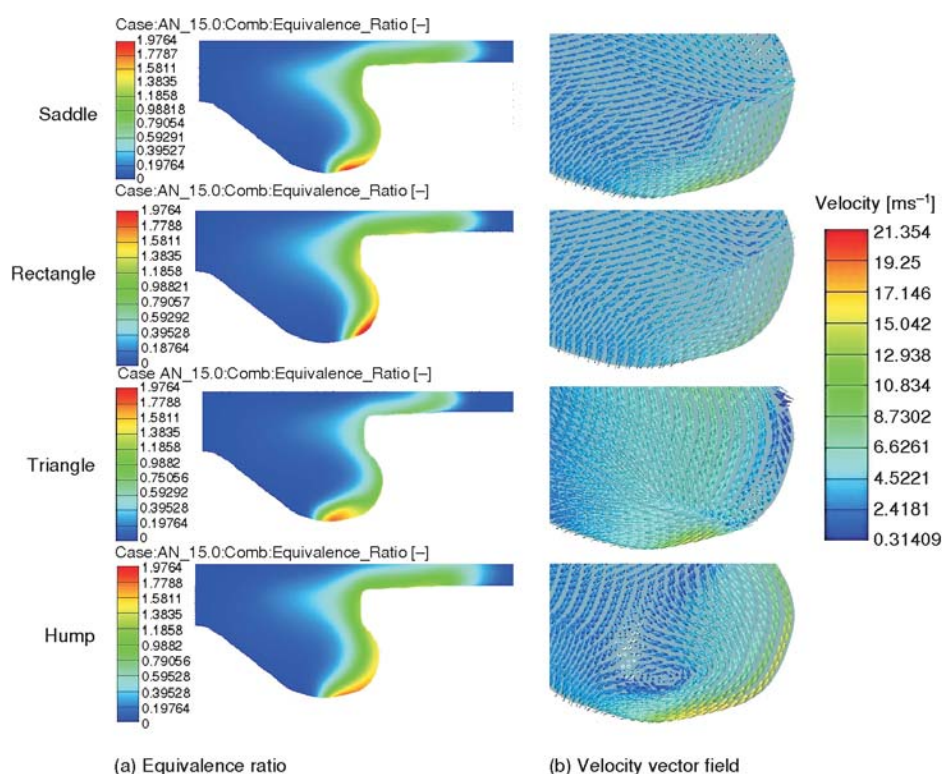


Figure 13. Distribution of equivalence ratio and velocity vector field  
(for color image see journal web site)

## Conclusions

- The numerical models for simulation of spray, combustion and emissions in the diesel chamber from a GM engine was setup and were validated through comparing the pressure and heat release in the cylinder calculated from the simulation with the experimental data.

- A new fuel injection rate shape named hump rate shape was come up with. Based on above validated numerical models, the numerical analysis of combustion and emission characteristics of the diesel engine with the new hump rate shape and other three different injection rate shapes, such as saddle, rectangle, and triangle rate shape were performed. The results showed that start of ignition for saddle and hump injection rate shapes comes earlier than that for triangle injection rate shape whose ignition delay was longest and combustion center was furthest away from TDC. Therefore, it is the triangle injection rate shape that had the lowest thermal efficiency in the four different injection rate shapes.
- For emission characteristics, more  $\text{NO}_x$  emission was produced for the saddle and hump injection rate shapes because of the larger high temperature area, which is the result of higher initial injection pressure leading to better atomization and shorter ignition delay period. Owing to the higher pressure in later injection period for the new hump injection rate shape, there is an obvious back flow to improve the mixing of fuel and air, so the soot emission for the hump injection rate shape was better than that for other shapes.

### Acknowledgments

This research was supported by the National Natural Science Foundation of China (No. 51176066, No.51276084) and A Project Funded by the Priority Academic Program Development of Jiangsu Higher Education Institutions.

### Nomenclature

$g_t$	– deceleration in the direction of travel, [m <sup>2</sup> s <sup>-2</sup> ]
$K_{RT}$	– wave number
$k$	– turbulence kinetic energy, [m <sup>2</sup> s <sup>-2</sup> ]
$L$	– turbulent length scale, [m]
$T$	– turbulent time scale, [s]
$\bar{v}^2$	– velocity scale, [ms <sup>-1</sup> ]

### Greek symbols

$\varepsilon$	– turbulent energy dissipation, [m <sup>2</sup> s <sup>-3</sup> ]
$\rho_g$	– density of gas, [kgm <sup>-3</sup> ]
$\rho_p$	– density of the droplet, [kgm <sup>-3</sup> ]
$\zeta$	– velocity scale ratio, [ms <sup>-1</sup> ]
$\Omega_{RT}$	– fastest growing frequency

### References

- [1] Zhou, L., *The Internal Combustion Engine* (in Chinese), 3<sup>rd</sup> ed., China Machine Press, Beijing, China, 2005
- [2] Masahiko, M., et al., Development of New Electronically Controlled Fuel Injection System ECD-U2 for Diesel Engines, SAE paper 910252, 1991, pp. 312-327
- [3] Furuta, K., et al., Study of the In-Line Pump System for Diesel Engines to Meet Future Emission Regulations, SAE paper 980812, 1998, pp. 125-136
- [4] Zhang, X., Turbocharged Diesel Engine Thermodynamic System Working Process Simulation (in Chinese), Ph. D. thesis, Dalian University of Technology, Dalian, China, 2011
- [5] Dambrosio, L., et al., VGT Turbocharger Controlled by Means of an Adaptive Control Technique, *Proceedings, IEEE/ASME International Conference on Advanced Intelligent Mechatronics*, Como, Italy, 2001, vol. 2, pp. 1087-1092
- [6] Mori, K., Worldwide Trends in Heavy-Duty Diesel Engine Exhaust Emission Legislation and Compliance Technologies, SAE paper 970753, 1997, pp. 19-29
- [7] Terry, B., Richards, P., A Method for Assessing the Low Temperature Regeneration Performance of Diesel Particulate Filters and Fuel-Borne Catalysts, SAE technical paper 2000-01-1922, 2000, pp. 1-5
- [8] Badami, M., et al., Influence of Multiple Injection Strategies on Emissions, Combustion Noise and BSFC of DI Common-Rail Diesel Engine, SAE technical paper 2002-01-0503, 2002
- [9] Suh, H., Investigations of Multiple Injection Strategies for the Improvement of Combustion and Exhaust Emissions Characteristics in a Low Compression Ratio (CR) Engine, *Applied Energy*, 88 (2011), 12, pp. 5013-5019

- [10] Sayin, C., et al., Effect of Injection Timing on the Exhaust Emissions of a Diesel Engine Using Diesel-Methanol Blends, *Renewable Energy*, 34 (2009), 5, pp. 1261-1269
- [11] Agarwal, K., et al., Effect of Fuel Injection Timing and Pressure on Combustion, Emissions and Performance Characteristics of a Single Cylinder Diesel Engine, *Fuel*, 111 (2013), September, pp. 374-383
- [12] Desantes, J. M., et al., The Modification of the Fuel Injection Rate in Heavy-Duty Diesel Engines, Part 1: Effects on Engine Performance and Emissions, *Applied Thermal Engineering*, 24 (2004), 17-18, pp. 2701-2714
- [13] Desantes, J. M., et al., The Modification of the Fuel Injection Rate in Heavy-Duty Diesel Engines, Part 2: Effects on Combustion, *Applied Thermal Engineering*, 24 (2004), 17-18, pp. 2715-2726
- [14] Shuai, S., et al., Evaluation of the Effects of Injection Timing and Rate-Shape on Diesel Low Temperature Combustion Using Advanced CFD Modeling, *Fuel*, 88 (2009), 7, pp. 1235-1244
- [15] Luckhchoura, V., Modeling of Injection-Rate Shaping in Diesel Engine Combustion, Ph. D. thesis, RWTH Aachen University, Aachen, Germany, 2010
- [16] Aggarwal, S., A Computational Study on the Effects of Pre-Ignition Processes on Diesel Engine Combustion and Emissions, *Proceedings*, 8<sup>th</sup> Thermal Engineering Joint Conference, Hawaii, USA, 2011 AJTEC2011-44202, pp. T20083-T20083-11
- [17] Hanjalić, K., et al., A Robust Near-Wall Elliptic-Relaxation Eddy-Viscosity Turbulence Model for CFD, *International Journal of Heat and Fluid Flow*, 25 (2004), 6, pp. 1047-1051
- [18] Durbin, P., Near-Wall Turbulence Closure without 'Damping Functions', *Theoretical and Comput. Fluid Dyn* (1991), 3, pp.1-13
- [19] \*\*\*, AVL Fire version 2011\_main program, 2011
- [20] \*\*\*, AVL Fire Product Description \_Turbulence modeling, 2011
- [21] \*\*\*, AVL Fire version 2011 \_Lagrangian Multiphase Module, 2011
- [22] Reitz, R.D., Diwakar, J, Effect of Drop Break-up on Fuel Sprays, SAE paper 860469, 1986
- [23] \*\*\*, AVL Fire version 2011 \_Combustion/Emission Module, 2011
- [24] Agafonov G., et al., Kinetic Modeling of Solid Carbon Particle Formation and Thermal Decomposition during Carbon Suboxide Pyrolysis behind Shock Waves, *Combust. Sci. and Techn.*, 174 (2002), 5-6, pp. 1-29
- [25] Appel, J., et al., Kinetic Modeling of Soot Formation with Detailed Chemistry and Physics: Laminar Premixed Flames of C2 Hydrocarbons, *Combust. Flame*, 121 (2000), 1-2, pp. 122-136
- [26] Evlampiev, et al., Global Kinetic Mechanisms for Calculation of Turbulent Reacting Flows: IV Diffusion Combustion, *Khim. Fiz.*, 20 (2001), 11, pp. 21-27
- [27] Kiefer, J., Sidhu, S., The Homogeneous Pyrolysis of Acetylene II: The High Temperature Radical Chain Mechanism, *Combust. Sci. and Techn.*, 82 (1992), 1-6, pp. 101-130
- [28] Krestinin A., Detailed Modeling of Soot Formation in Hydrocarbon Pyrolysis, *Combust. Flame*, 121 (2000), 3, pp. 513-524
- [29] Haynes, B. S., Wagner, H. Gg., Soot Formation, *Progress Energy Combustion Science*, 7 (1981), 4, pp. 229-273
- [30] Wagner, H., Vlasov, P., The Kinetics of Carbon Cluster Formation during C<sub>3</sub>O<sub>2</sub> Pyrolysis, *Kinetics and Catalysis*, 42 (2001), 5, pp. 645-656
- [31] Wang, H., Su, W., A Study of Realization of Modulated Multi-Pulse Injection Mode and Its Effects on HCCI Combustion (in Chinese), *Transactions of CSICE*, 23 (2005), 5, pp. 385-391
- [32] He, X., The Determination Methods of the Start and End Point of Combustion in Diesel Engine (in Chinese), *Acta Armamentarii* (1988), 2, pp. 27-33
- [33] We, H., et al., Effect of Transient Conditions on Combustion Noise of Internal Combustion Engines (in Chinese), *Chinese Internal Combustion Engine Engineering*, 27 (2006), 2, pp. 54-60
- [34] Wei, H., Stimulation Mechanism of Combustion Noise in Transient Condition of DI-Diesel Engine (in Chinese), Ph. D. thesis, Tianjin University, Tianjin, China, 2004